DOI 10.2478/ama-2019-0005

STATIC ELECTROMECHANICAL CHARACTERISTICS OF PIEZOELECTRIC CONVERTERS WITH VARIOUS THICKNESS AND LENGTH OF PIEZOELECTRIC LAYERS

Grzegorz MIECZKOWSKI*

*Faculty of Mechanical Engineering, Białystok University of Technology, ul. Wiejska 45C, 15-351 Białystok, Poland

g.mieczkowski@pb.edu.pl

received 10 July 2018, revised 10 March 2019, accepted 15 March 2019

Abstract: The paper presents the analysis of electromechanical characteristics of piezoelectric converters subjected to an electric field and mechanical load. The analyses were performed based on a method consisting implementation of special segments responsible for electrical boundary conditions to a homogeneous beam. Constitutive equations were developed, allowing one to obtain static electromechanical characteristics for piezoelectric actuators with freely defined boundary conditions and geometry. Moreover, based on constitutive equations obtained, a particular solution for cantilever transducer subjected to concentrated force has been developed. The resulting analytical solution was compared with the data available in the literature, and the developed FEM solution. Furthermore, the influence of factors such as relative length, thickness and location of particular piezoelectric layers on electromechanical characteristics of the transducer was defined.

Key words: Piezoelectric bender, constitutive equations, deflection, electromechanical characteristics

1. INTRODUCTION

Today piezoelectric transducers are applied in many different industries (Tzou, 1999; Przybyłowicz, 1999; Liu et al., 2014, Szpica et al., 2018). They are used as measuring and controlling elements in, more or less complex, systems for working process execution. Design of a transducer depends on its manufacturing method and intended use. Normally, they are made of one or more piezoelectric layers (with electrodes placed on their entire length) and a non-piezoelectric component. Their working principle is based on the conversion of electric energy to mechanical, or vice versa (Busch-Vishniac, 1999). Electromechanical characteristics – relation between deflection of a transducer and applied electrical and mechanical loads, is defined based on constitutive equations. These equations bound together geometrical properties, material properties and physical parameters, such as force, displacement and electric field. Developing and solving of such simultaneous equations, in case of piezoelectric benders, is very difficult. Material and geometrical heterogeneity of the global structure of bender and diverse boundary conditions force the use of some reductions.

Electromechanical characteristics of piezoelectric transducers were dealt with by many scientists. Smits et al. (1991), by using energetic methods, formed and solved physical equations for a transducer made of two layers of even length (piezoelectric bimorph). Then Wang and Cross (1999) extended and solved the issue of a triple segment, while Xiang and Shi (2008) – a multilayer one. In papers (Park and Moon, 2005; Dunsch and Breguet, 2008; Rahmoune and Osmont, 2010; Raeisifard et al., 2014, Mieczkowski, 2016, Nguyen et al., 2018), results of piezoelectric bimorph testing were given, wherein their design featured piezoelectric layer of length other than that of a non-piezoelectric component. The paper (Mieczkowski, 2017) analysed static and dynamic characteristics of a three-layer actuator, made of a non-piezoelectric component and two piezoelectric layers of the same length and thickness. Durability and utility features of piezoelectric transducer were analysed in paper (Mieczkowski, 2018).

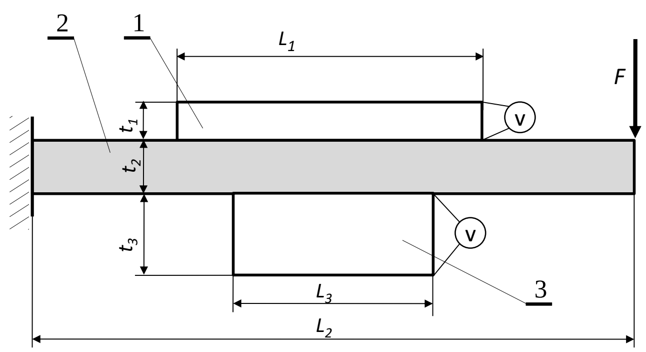

Fig. 1. Three-layer piezoelectric converter; 1,3 – piezoelectric elements, 2 – beam

The paper presents tests performed in a way similar to those given in the paper (Mieczkowski, 2017), extending them by a possibility to include, within constitutive equations, the diversity of thickness and length of particular piezoelectric layers (Fig. 1).

The other objective of researching was to determine the influence of relative thickness, length and location of particular piezoelectric layers on electromechanical characteristics of transducers. Therefore, based on the constitutive equations defined, a particular solution for cantilever transducer (subjected to concentrated force) was developed and necessary analyses were made allowing one to determine the influence of the above parameters on its electromechanical characteristics.

2. CONSTITUTIVE EQUATIONS

2.1. Basic assumptions

To define constitutive equations, the method (described in detail in papers [Mieczkowski, 2016; Mieczkowski, 2017]), which allows for implementation to a homogeneous beam two types of modules, hereinafter referred to as PBS (piezoelectric bimorph segment) and PTS (piezoelectric triple segment) was used. This allows for including in electromechanical characteristics of the segment a local change in stiffness and strain, which are caused by the transverse piezoelectric effect (Curie et al., 1880). In order to reduce the mathematical model, the following assumptions were made:

a) bending of the element takes place according to the Euler's hypothesis, and radii of curvature of the deflected components are identical
b) in connection plane of piezoelectric and non-piezoelectric components, there is no intermediate layer (the presence of adhesive layers and electrodes on the bottom and top surface of the piezoelectric material is omitted), and no sliding occurs,
c) in piezoelectric layers, transverse piezoelectric effect 1–3 takes place, causing pure bending.

2.2. General equation for strain of piezoelectric triple segment

Fragment of three-layer piezoelectric converter, as given in Fig. 2, shall now be examined. In the structure of the transducer, two piezoelectric components (of different thickness and length) and a non-piezoelectric element can be distinguished. Moment *M(x)* is induced by mechanical operating load. Its value and distribution is also dependant on boundary conditions related to the mounting of the converter. In the bender, also electrical load M_{ei} will occur, caused by piezoelectric effect (present in piezoelectric components).

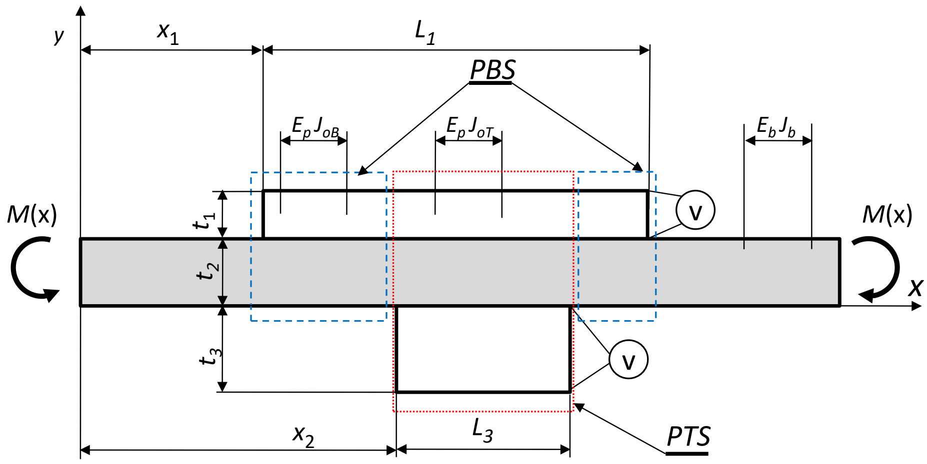

Fig. 2. Fragment of three-layer piezoelectric converter

In the analysed structure, subjected to bending, it is possible to determine the five characteristic ranges, related to a change in load and stiffness. Within the $x_1<x<x_2$ and $x_2+L_3<x<x_1+L_1$ ranges, there is a piezoelectric bimorph segment *PBS* (generating electric moment M_{eB}) with flexural stiffness E_pJ_{oB}. Between the *PBS* segments (the $x_2<x<x_2+L_3$ segment), there is piezoelectric triple segment *PTS*, which generates electric moment M_{eT} and has flexural stiffness E_pJ_{oT}. The other two ranges are within the homogeneous beam with stiffness E_bJ_b.

Taking into account the above structural variability and load conditions, general differential equation for strain of bender can be noted as follows:

$$\frac{\partial^2 y}{\partial x^2}=M_{eB}\,\gamma_B\begin{pmatrix}(H[x-x_1]-H[x-x_2])+\\+(H[x-(x_2+L_3)]-H[x-(x_1+L_1)])\end{pmatrix}+ \\ +M_{eT}\,\gamma_T(H[x-x_2]-H[x-(x_2+L_3)])+M(x)/\mathrm{E_b}J_\mathrm{b} \quad (1)$$

where: $H[x-x_i]$ – Heaviside function,
$\gamma_B=\frac{E_bJ_b(M_{eB}+M(x))-E_pJ_{oB}M(x)}{E_bJ_bE_pJ_{oB}M_{eB}}\gamma_T=\frac{E_bJ_b(M_{eT}+M(x))-E_pJ_{oT}M(x)}{E_bJ_bE_pJ_{oT}M_{eT}}$ – factors including change in stiffness with applied formal notation of the Heaviside function, E_p, E_b – Young's modules of piezoelectric and non-piezoelectric element, J_b, J_{oB}, J_{oT} – moments of inertia (described hereinafter).

As the determining of the mechanical moment $M(x)$ in general does not pose any problems, determining electric load Mei, generated by piezoelectric segments, is very burdensome and requires solving the two-dimensional problem of bending the multilayer structure, while taking piezoelectric effect into account.

2.3. Electric load M_{ei} generated by piezoelectric segments

2.3.1. Piezoelectric triple segment *PTS*

Three-layer structure of piezoelectric triple segment *PTS* (Fig. 3), with constant width *b*, made of two piezoelectric components (1) and (3) and a non-piezoelectric element (2), shall now be investigated.

The *PTS* is not subjected to any mechanical load, and longitudinal forces N_i and bending moments M_i occurring on individual layers are the result of the applied voltage V. Based on the equilibrium equation of forces condition, the following can be noted:

$$N_1+N_2+N_3=0. \quad (2)$$

The sum of moments in relation to interface must be zero, therefore:

$$M_1+M_2+M_3-\frac{N_2t_2}{2}-N_3\left(t_2+\frac{t_3}{2}\right)+\frac{N_1t_1}{2}=0. \quad (3)$$

DOI 10.2478/ama-2019-0005

According to the adopted Euler's hypothesis, bending moments can be notified as follows:

$$\begin{cases} M_1 = \frac{E_p J_{p1}}{\rho} \\ M_2 = \frac{E_b J_b}{\rho} \\ M_3 = \frac{E_p J_{p3}}{\rho} \end{cases}. \tag{4}$$

Substituting relations (4) to (3) and providing simple mathematical transformations resulted in the following:

$$\frac{1}{\rho} = \frac{(N_2+2N_3)t_2 - N_1 t_1 + N_3 t_3}{2\left(E_b J_b + E_p J_{p1} + E_p J_{p3}\right)}. \tag{5}$$

Including the relation between radius of curvature ρ and deflection $w(x)$:

$$\frac{1}{\rho} = \frac{\partial^2 w}{\partial x^2}, \tag{6}$$

differential equation for bending of converter can be notified as follows:

$$\frac{\partial^2 w}{\partial x^2} = \frac{(N_2+2N_3)t_2 - N_1 t_1 + N_3 t_3}{2\left(E_b J_b + E_p J_{p1} + E_p J_{p3}\right)} \tag{7}$$

Constitutive equations for lower and upper converter layers, including the piezoelectric effect in layers 1 and 3 gave the following:

$$\begin{cases} \frac{\partial u_{x1}}{\partial x} = \frac{N_1}{E_p A_{p1}} - d_{31}\left(\frac{-V}{t_1}\right) \\ \frac{\partial u_{x2}}{\partial x} = \frac{N_2}{E_b A_b} \\ \frac{\partial u_{x3}}{\partial x} = \frac{N_3}{E_p A_{p3}} + d_{31}\left(\frac{-V}{t_3}\right) \end{cases}, \tag{8}$$

where: A_b, A_{p1}, A_{p3} – layers cross sectional areas, d_{31} – piezoelectric constant.

Following the displacement continuity condition (Fig. 3), it was found that:

$$\begin{cases} u_{x1} - u_{x2} - \frac{\partial w}{\partial x}\left(\frac{t_1}{2} + \frac{t_2}{2}\right) = 0 \\ u_{x1} - u_{x3} - \frac{\partial w}{\partial x}\left(\frac{t_1}{2} + \frac{t_3}{2} + t_2\right) = 0 \end{cases}. \tag{9}$$

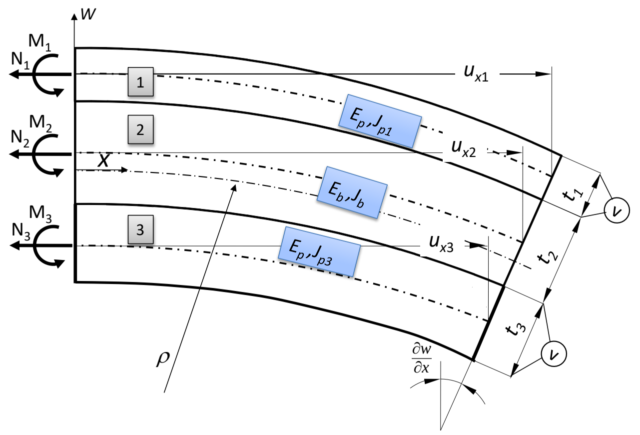

Fig. 3. Distribution of forces and conditions for strain of piezoelectric triple segment *PTS*

Solving of differential equations (7) and (8), with the following boundary conditions:

$$\begin{cases} \frac{\partial w}{\partial x}(0) = 0, w(0) = 0 \\ u_{x1}(0) = 0, u_{x2}(0) = 0, u_{x3}(0) = 0 \end{cases}, \tag{10}$$

and by applying relation (9), longitudinal force N_i can be determined:

$$\begin{cases} N_1 = -\frac{b d_{31} E_p V\left(\alpha_3 + E_b E_p t_2\left(t_1^3 + t_2^2(4t_1 - 2t_3) + 3t_1^2 t_3 - 2t_3^3 + 3t_2(t_1 - t_3)(t_1 + 2t_3)\right)\right)}{\alpha_1 + \alpha_2} \\ N_2 = -\frac{-3 b d_{31} E_b E_p^2 V t_2 (t_1 - t_3)(t_2 + t_1 + t_3)(2t_2 + t_1 + t_3)}{\alpha_1 + \alpha_2} \\ N_3 = \frac{b d_{31} E_p V\left(\alpha_3 + E_b E_p t_2\left(-2t_1(t_2^2 + 3t_2 t_1 + t_1^2) + t_2(4t_2 + 3t_1)t_3 + 3(t_2 + t_1)t_3^2 + t_1^3\right)\right)}{\alpha_1 + \alpha_2} \end{cases} \tag{11}$$

where: $\alpha_1 = E_b{}^2 t_2{}^4 - 2E_b E_p t_2(t_1{}^3 + t_3{}^3 + t_2{}^2(t_1 + t_3) + 3t_2(t_1{}^2 + t_3{}^2))$, $\alpha_2 = E_p{}^2(t_1{}^4 - 2t_1{}^3 t_3 + t_3{}^4 - 6t_1{}^2 t_3(2t_2 + t_3) - 2t_1 t_3(6t_2{}^2 + 6t_2 t_3 + t_3{}^2)$, $\alpha_3 = E_b{}^2 t_2{}^4 + E_p{}^2(t_1{}^4 + t_1{}^3 t_3 + t_1 t_3{}^3 + t_3{}^4)$.

The differential equation for bending of *PTS,* in the M_{eT} moment function, can be notified as follows:

$$\frac{\partial^2 w}{\partial x^2} = \frac{-M_{eT}\left(1 + \frac{t_2}{t_1 + t_3}\right)}{E_p J_{oT}}. \tag{12}$$

Basing on the comparison of relations (7) and (12), it is possible to determine the bending moment M_{eT}, which is the result of the piezoelectric effect:

$$M_{eT} = \frac{E_p J_{oT}(t_1 + t_3)(N_1 t_1 - N_2 t_2 - 2N_3 t_2 - N_3 t_3)}{2\left(E_b J_b + E_p J_{p1} + E_p J_{p3}\right)(t_1 + t_2 + t_3)}. \tag{13}$$

The required moment, taking relation (11) into account, can be noted as follows:

$$M_{eT} = d_{31} E_p{}^2 V \theta, \tag{14}$$

where:

$$\theta = \frac{-b\, J_{oT}(t_1 + t_3)(t_1 + 2t_2 + t_3)\left(E_b t_2 + E_p(t_1 + t_3)\right)\left(E_b t_2{}^3 + E_p(t_1{}^3 + t_3{}^3)\right)}{2\left(E_b J_b + E_p J_{p1} + E_p J_{p3}\right)(t_1 + t_2 + t_3)(\alpha_1 + \alpha_2)}.$$

Moments of inertia for particular layers are, respectively:

$$J_b = \frac{b t_2^3}{12}, J_{p1} = \frac{b t_1^3}{12}, J_{p3} = \frac{b t_3^3}{12}. \tag{15}$$

The averaging value of the moment of inertia JoT (16) – calculated in relation to the neutral layer – was determined in the same way as in the paper (Mieczkowski, 2016), using the method of transformation of the cross sectional area (Fertis, 1996).

$$\begin{gathered} J_{oT} = \frac{b(\alpha_1 + \alpha_2 + \alpha_4)}{12 E_p\left(E_b t_2 + E_p(t_1 + t_3)\right)}, \\ \alpha_4 = 6E_p(E_p t_1 t_3(t_1 + 2t_2 + t_3)^2 + \\ E_b t_2(t_1{}^3 + 2t_1{}^2 t_2 + t_1 t_2{}^2 + t_3(t_2 + t_3)^2)) \end{gathered} \tag{16}$$

2.3.2. Piezoelectric bimorph segment *PBS*

Solution for the issue of piezoelectric bimorph segment is provided in the paper (Mieczkowski, 2016). Below are the relations describing electric load (17) generated by the *PBS* and the averaging value of the moment of inertia (18).

$$M_{eB} = d_{31}E_p{}^2V\beta, \tag{17}$$

$$J_{oB} = \frac{b\beta_2}{12E_p(E_bt_2+E_pt_1)}, \tag{18}$$

where: $\beta = \frac{6E_bJ_{oB}t_2(t_2+t_1)}{\beta_2}, \beta_2 = E_b{}^2t_2^4 + E_p{}^2t_2^4 + 2E_bE_pt_2t_1(2t_2^2 + 3t_2t_1 + t_1^2)$.

2.4. Electromechanical characteristics of cantilever transducer subjected to concentrated force *F*

This part of the paper is concerned with the application of the proposed method, based on implementing the *PBS* and *PTS* segments to a homogeneous beam so as to determine the analytical relations describing the deflection of the transducer with fixed geometry and known boundary conditions.

In the transducer, as shown on Fig. 4, the left side is fixed-mounted, and the right can move freely. The operational load results from the external force *F* and electric moments M_{ei} generated by the applied voltage V. Based on the conditions for equilibrium of forces and moments, values for the reaction in mounting were established, and are as follows: $R_y = \mathrm{F}, R_x = 0, M_F = FL$.

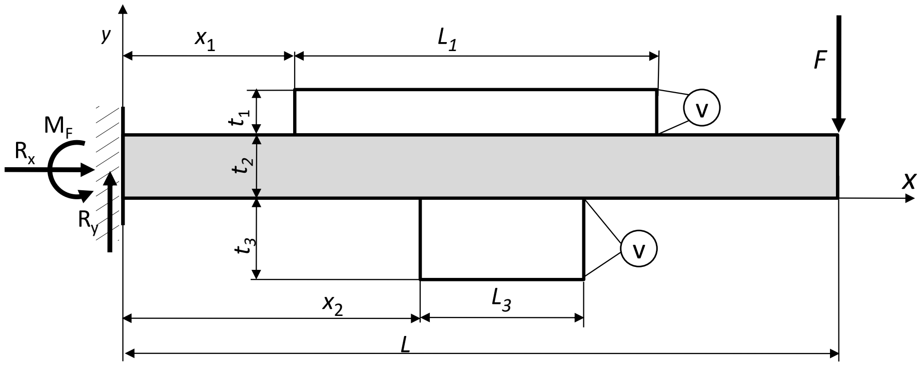

Fig. 4. Cantilever transducer with *PBS* and *PTS* segments

Therefore, mechanical moment *M*(*x*) takes the following form:

$$M(x) = -M_F + R_yx = -FL + Fx. \tag{19}$$

Substituting relations (14), (17) and (19) to the general solution, described by the formula (1), upon double integration, gives a relation that describes deflection of the analysed bender (20):

$$y(x) = \frac{1}{6E_bE_pJ_bJ_{oB}\,J_{oT}}(A_1v + B_1F), \tag{20}$$

where:

$$A_1 = 3E_bd_{31}E_p^2J_b + \{\beta J_{oT}H[x-x_1](x-x_1)^2 - (\beta J_{oT} - \theta J_{oB})(H[x-x_2](x-x_2)^2 + x(L_3+x_2)^2)$$
$$+H[x-L_3-x_2](L_3-x+x_2)^2 - \beta J_{oT}H[x-L_1-x_1](L_1-x+x_1)^2\},$$

$$B_1 = J_{oT}\big(E_pJ_{oB} - E_bJ_b\big)(H[x-x_1](x-x_1)^2(3L-x-2x_1) - H[x-x_1-L_1](3L-2L_1-x-2x_1)(L_1-x+x_1)^2)$$
$$+E_pJ_{oB}J_{oT}x^2(x-3L) + (J_{oB}-J_{oT})E_bJ_b\begin{pmatrix}-H[x-x_2](x-x_2)^2(3L-x-2x_2) + (2(L_3+x_2)-3L)(L_3+x_2)^2x \\ +H[x-x_2-L_3](3L-2L_3-x-2x_2)(L_3-x+x_2)^2\end{pmatrix}.$$

Integration constants are determined on the basis of the following boundary conditions:

$$\frac{\partial y}{\partial x}(0) = 0, y(0) = 0. \tag{21}$$

It is worth noting that, in the obtained solution (20), assumption of even length ($L_1 = L_3$) and thickness ($t_1 = t_3$) of both piezoelectric layers, results in obtaining the identical solution as the one presented in the paper (Mieczkowski, 2017). In order to determine the electromechanical behaviour of the converter, most frequently, the FEM-based analyses are carried out (Rahmoune and Osmont, 2010, Szpica, 2015, 2018, Borawski, 2015, 2018). Therefore, in order to validate the method developed, a transducer with the following geometry – $L_1 \neq L_3$, $t_1 \neq t_3$ – was modelled following the *FEM* method with the use of the ANSYS application (Mieczkowski, 2016; Documentation for ANSYS, 2010). In the calculations, the following material data were assumed:

- Young's modulus: E_p = 2.0’10[9], E_b = 4.0’10[9], N/m[2]
- Poisson's ratio: υ_p = 0.29, υ_b = 0.33
- Piezoelectric strain coefficients: d_{31} = 2.2’10[-11] C/N, d_{32} = 0.3’10[-11] C/N, d_{33} = -3.0’10[-11]C/N
- Relative permittivity at constant stress: $(\varepsilon_{33})^T = 12$

The difference between analytical and numerical solutions was approx. 1% for electrical load and 3% for mechanical load. The comparison of both solutions is graphically shown in Fig. 5.

The obtained particular solution (20) allowed one to determine the influence of mutual geometric relations of particular components of the bender on its functional characteristics. Two types of converters were analysed:

1. converter with piezoelectric components of different length – $L_1 \neq L_3$ (whereas the upper piezoelectric layer is of the same length as beam element – $L_1 = L$)
2. two piezoelectric layers of the same length – $L_1 = L_3$, $x_1 = x_2$

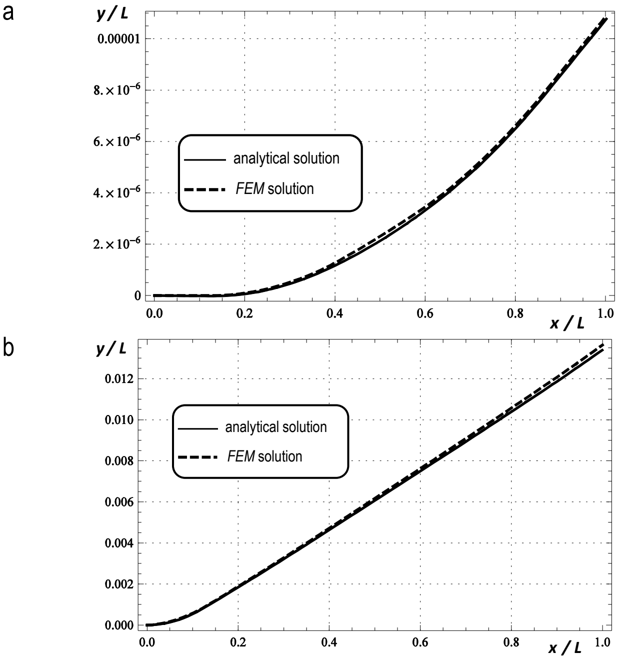

Fig. 5. Deflection of the cantilever converter for x_1 = 0, x_2 = 2/3L, t_1 = 2 mm, t_2 = 1 mm, t_3 = 6 mm, L = 60 mm: a) subjected only to an electrical voltage, V = 100 V, F = 0; b) subjected only to a force, V = 0, F = -10N

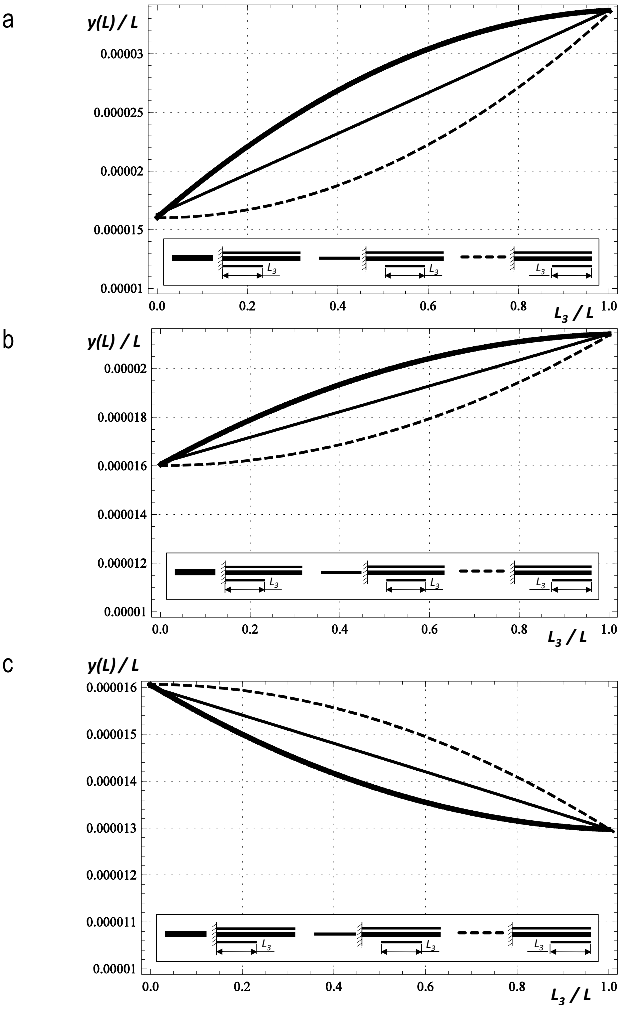

Fig. 6. Influence of location and length of the piezoelectric element on the deflection of the transducer under electric load (v = 100 V, F = 0) only; a) t_1/t_3 = 2, b) t_1/t_3 = 1, c) t_1/t_3 = 0.5

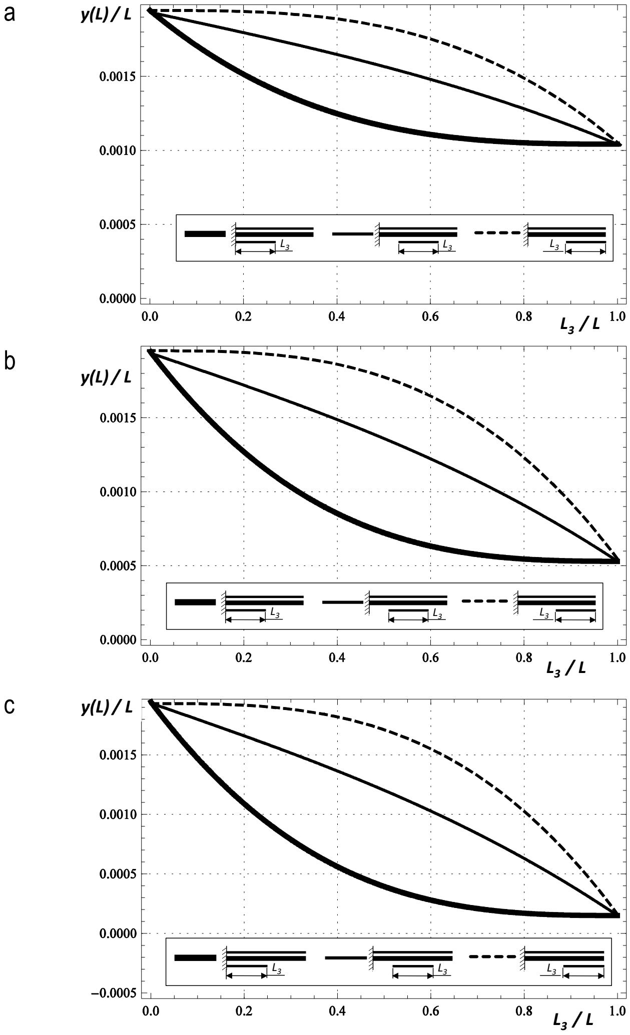

Fig. 7. Influence of location and length of the piezoelectric element on the deflection of the transducer under mechanical load (F = -10 N, V = 0) only; a) t_1/t_3 = 2, b) t_1/t_3 = 1, c) t_1/t_3 = 0.5

For both variants, the influence of the above parameters on the deflection of the right end of the transducer was analysed:

- relative thickness of particular piezoelectric elements t_1/t_3
- relative length of components $L_{1,3}/L$
- locations of piezoelectric components (*PTS* segment: at the left of the converter -x_2 = 0, in the middle - $x_2 + L_3/2 = L/2$, at the right - $x_2 + L_3 = L$)

In the analysis performed, the following material and geometric data were included: $E_{\mathrm{p}} = 2.0'10^{9}$ N/m^2, $E_{\mathrm{b}} = 4.0'10^{9}$ N/m^2, $d_{31} = 2.2'10^{-11}$ C/N, L = *60* mm, t_2 = 1 mm.

The below figures show a graphical representation of the results of tests carried out for the converter with different length of piezoelectric components, subjected to electric moment (Fig. 6) and mechanical load (Fig. 7).

Based on the obtained results (Fig. 6), it can be claimed that when subjecting the element to electric moment only, displacement of the right end of the transducer:

- is increased with the increase in relative thickness of the layers t_1/t_3
- is increased with the increase in relative length L_3/L in case of $t_1/t_3 \geq 1$

DOI 10.2478/ama-2019-0005 acta mechanica et automatica, vol.13 no.1 (2019)

- is decreased with the increase in relative length L_3/L in case of $t_1/t_3 < 1$
- has the highest value, when the piezoelectric segment is located at the left in case of $t_1/t_3 \geq 1$
- has higher values ($L_3 \neq 0$, $L_3 \neq L$), when the piezoelectric segment is located at the right in case of $t_1/t_3 < 1$

As expected, when applying mechanical load only (Fig. 7), the increase in relative thickness of layers t_1/t_3 causes the increase in the deflection of the transducer. The biggest displacement is achieved, when the piezoelectric segment is located at the right of the transducer. Noticeable also is the decrease in displacement value along with the increase in the L_3/L parameter value.

The results of analyses for the transducer with piezoelectric layers of the same length ($L_1 = L_3$, $x_1 = x_2$), are given in Fig. 8. Due to the fact that when applying mechanical load, the influence of the considered factors (relative thickness, length and location of piezoelectric layers) on electromechanical characteristics was identical as in the case of the converter with different lengths of piezoelectric components, the results obtained only for electric load are given.

a

b

c

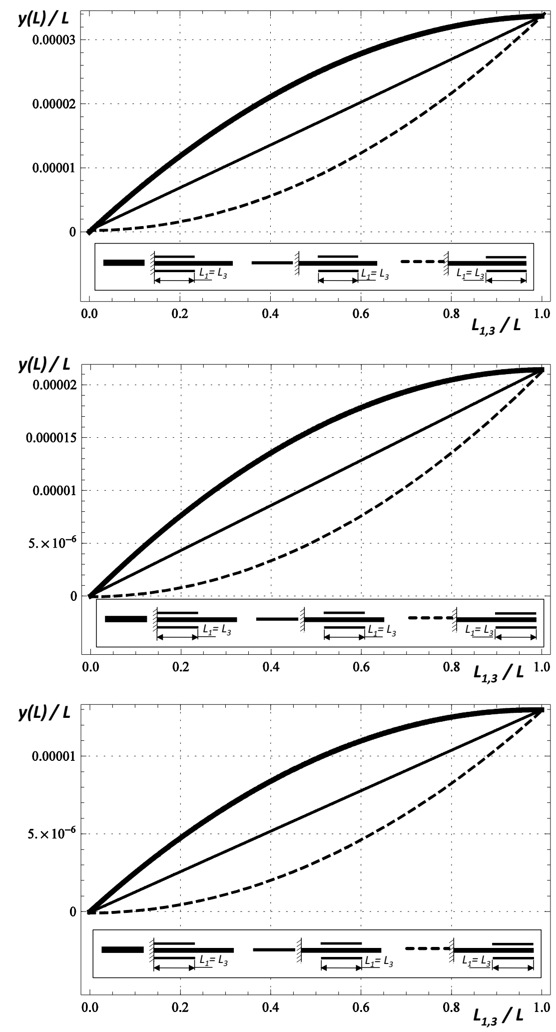

Fig. 8. Influence of location and length of the piezoelectric element on the deflection of the transducer – with the same length of piezoelectric components – under electric load (v = 100 V, F = 0) only; a) $t_1/t_3 = 2$, b) $t_1/t_3 = 1$, c) $t_1/t_3 = 0.5$

Analysing the obtained results, as given in Fig. 8, it can be claimed that displacement of the right end of the transducer increases with the increase in relative thickness (t_1/t_3) and length ($L_{1,3}/L$) of piezoelectric layers. The highest values of relocation are obtained when piezoelectric segment is located at the left.

3. CONCLUSIONS

Based on the testing performed, it can be noted that:

- the obtained solution for cantilever transducer, assuming the same length and thickness of piezoelectric layers, is compatible with the solution provided in paper (Mieczkowski, 2017)
- analytical solutions conform to the results obtained from the *FEM* (for electric load, the difference is about 1%, and for mechanical load – 3%)

As for the electromechanical characteristics of the cantilever transducer, it was found that the following factors have significant influence on the conditions of strain of the transducer:

- relative thickness of particular piezoelectric elements t_1/t_3
- relative length of components $L_{1,3}/L$
- locations of piezoelectric components

For transducer with different length of piezoelectric layers, displacement of the end of the transducer is increased with the increase in relative thickness of the layers t_1/t_3. Increase in relative length L_3/L results in:

a) when applying electric load:
   - increase in displacement $y(L)$, if $t_1/t_3 \geq 1$
   - decrease in displacement $y(L)$, if $t_1/t_3 < 1$
b) when applying mechanical load:
   - decrease in displacement

The biggest relocation ($L_3 \neq 0$, $L_3 \neq L$) is achieved when piezoelectric segment is located:

a) when applying electric load:
   - at the left in case of $t_1/t_3 \geq 1$
   - at the right in case of $t_1/t_3 < 1$
b) when applying mechanical load:
   - at the right of the transducer

Analysing the issue of the transducer with uniform length of piezoelectric layers, it was found that:

a) for applying mechanical load, the influence of the considered factors on electromechanical characteristics was identical to the case of the transducer with different lengths of piezoelectric components
b) when applying electric load (induced by the voltage V):
   - deflection of the right end of the transducer is increased with the increase in relative thickness (t_1/t_3) and length ($L_{1,3}/L$) of piezoelectric layers
   - the highest values of displacement are achieved in the case when piezoelectric segment is located at the left

It is therefore concluded that the utility features of the piezoelectric transducers are significantly influenced by their geometrical properties. The increase in thickness and length of piezoelectric layers increases the flexural stiffness and the generated moment M. The increase in stiffness results in a decrease in converter deflection. However, the increase in the moment increases its deflection. Therefore, by choosing the location, thickness and length of the piezoelectric components properly, a compromise solution can be obtained, ensuring the greatest deflection of the transducer. Analytical solutions describing deformations of piezoelectric transducers may be helpful in this.

REFERENCES

1. **Borawski A.** (2015), Modification of a fourth generation LPG installation improving the power supply to a spark ignition engine, *Eksploatacja i Niezawodnosc* (*Maintenance and Reliability*), 17(1), 1–6.
2. **Borawski A. (**2018), Simulation study of the process of friction in the working elements of a car braking system at different degrees of wear, *Acta Mechanica et Automatica*,12(3), 221–226.
3. **Busch-Vishniac I.J.** (1999), *Electromechanical Sensors and Actuators*, Springer-Verlag.
4. **Curie P.J., Curie J.** (1880), *Crystal Physics-Development by Pressure 0/ Polar Electricity in Hemihedral Crystals with Inclined Faces*, Acad. Sci.(Paris) C. R. Hebd. Seances, 91, 294 (in French).
5. **Documentation for ANSYS, Coupled-Field Analysis Guide** (2010).
6. **Dunsch R., Breguet J.M. (**2006), Unified mechanical approach to piezoelectric bender modelling, *Sens. Actu.* 134, 2, 436–446.
7. **Fertis D.G.** (1996), *Advanced Mechanics of Structures*, Marcel Dekker, New York.
8. **Liu X., Wang X., Zhao H., Du Y.** (2014), Myocardial cell pattern on piezoelectric nanofiber mats for energy harvesting, J*. Phys: Conf. Ser*. 557, 1–5.
9. **Mieczkowski G.** (2016), Electromechanical characteristics of piezoelectric converters with freely defined boundary conditions and geometry, *Mechanika*, 22(4), 265–272.
10. **Mieczkowski G.** (2017), The constituent equations of piezoelectric cantilevered three-layer actuators with various external loads and geometry, *Journal of Theoretical and Applied Mechanics*, 55(1), 69–86.
11. **Mieczkowski G.** (2018), Optimization and Prediction of Durability and Utility Features of Three-Layer Piezoelectric Transducers, *Mechanika*, 24(3), 335–342.
12. **Nguyeni V-T., Kumar P., Leong J.Y.C.** (2018), Finite Element Modelling and Simulations of Piezoelectric Actuators Responses with Uncertainty Quantification, *Computation,* 6(4), 1–20.
13. **Park J.K., Moon W.K.** (2005), Constitutive relations for piezoelectric benders under various boundary conditions, *Sens. Actuat. A*, 117, 159–167.
14. **Przybyłowicz P.M.** (1999), Application of piezoelectric elements to semi-adaptive dynamic eleminator of torsional vibration, *Journal of Theoretical and Applied Mechanics*, 37, 2, 319-334.
15. **Puławski G., Szpica D.** (2015), The modelling of operation of the compression ignition engine powered with diesel fuel with LPG admixture, *Mechanika*, 21(6), 501-506.
16. **Raeisifard H. Bahrami M.N. Yousefi-Koma A., Fard H. R.** (2014), Static characterization and pull-in voltage of a micro-switch under both electrostatic and piezoelectric excitations, *European Journal of Mechanics A/Solids*, 44, 116-124.
17. **Rahmoune M., Osmont D.** (2010), Classic finite elements for simulation of piezoelectric smart structures, *Mechanika*, 86(6), 50-57.
18. **Smits J.G., Dalke S.I., Cooney T.K.** (1991), The constituent equations of piezoelectric bimorphs, *Sensors and Actuators A*, 28, 41–61.
19. **Ştefănescu D. M.** (2011), Piezoelectric Force Transducers (PZFTs), *Handbook of Force Transducers*, 109-130.
20. **Szpica D.** (2018), Modeling of the operation of a Dual Mass Flywheel (DMF) for different engine-related distortions, *Mathematical and Computer Modelling of Dynamical Systems*, 24(6), 643-660.
21. **Szpica D., Borawski A., Mieczkowski G.** (2018), New Concept of Low-Pressure Gas-Phase Injector, *Proceedings of the 23nd International Scientific Conference*, 173-176.
22. **Tzou H.S.** (1999), *Piezoelectric Shells: Distributed Sensing and Control of Continua*, Kluwer Academic Publishers, Dordrecht.
23. **Wang Q., Cross L.E**. (1999), Constitutive equations of symmetrical triple-layer piezoelectric benders, *IEEE Trans. Ultrason. Ferroelec.Freq. Contr.*, 46, 1343–1351.
24. **Xiang H.J., Shi Z.F**. (2008), Static analysis for multi-layered piezoelectric cantilevers, *International Journal Of Solids And Structures*, 45(1), 113-128.

Studies were carried out within work no. S/WM/1/18 and funded from under development of science by Ministry of Science and Higher Education.